NOTA INFN-19-04/MI_BI

Low cost SiPM-based detector for the measurement of the energy loss of a proton beam, with particular focus on the Bragg peak

V. Pagliarino[a], F. Serra[a], A. Robino[a], F. Filippa[a], R. Ponte[a], G. Branda[a], A. Massolino[a], A. Lovisolo[a], F. Boido[a]

a. Scientific High School "Galileo Galilei" part of I.I.S. "Nicola Pellati" – Nizza Monferrato (AT) - Italy

Article Info

Keywords:
Bragg Peak
Low cost detectors
Scintillators and SiPM
Protontherapy
Proton beam
Educational

Abstract

Nowadays, thanks to the spreading of different applications in the field of applied nuclear physics, such as protontherapy, detector testing and radiation hardness measurement, the number of particle beam facilities all around the world is significantly growing and the characterisation of these beams is becoming a very frequent operation. Here we present a low cost detector, made up by a student team selected by the Italian Institute for Nuclear Physics, for the study of the energy loss curve of charged particle beams, employing scintillator and SiPM technology, that allows both to make quick measurements without a complex setup and to run experiments for educational purposes, thanks to its expandable design.

1. Introduction

The P.R.O.ME.THE.U.S.[1] experiment is a particle detector designed and built by a team of students of the I.I.S. "Nicola Pellati" Scientific High School, shortlisted in the CERN Beamline for School 2017 competition. This machine, thanks to the precious collaboration with the Italian National Institute for Nuclear Physics has been tested on a particle accelerator at the proton cyclotron facility managed by the Trento Institute for Fundamental Physics and Applications in Italy. The P.R.O.ME.THE.U.S. detector employs scintillators and the silicon photomultiplier (SiPM) technology to study the charged particles energy loss, with particular focus on the Bragg Peak. A large variety of particles could be used, ranging from protons to different kind of ions in a large spectrum of compatible energies; in our measurements we used a 150 MeV proton beam. This detector can be used for different kinds of beam characterisation, in particular for proton or ion beams employed in particle therapy. This machine was not designed for high precision measurements, but represents an interesting example of a detector project that allows to perform quick acquisitions, reaching a good level of performance with a significantly lower cost for machine construction and maintenance. The prospects of usage of this detector also include studies of the SiPM behaviour itself, comparison studies of scintillators, specifically for protontherapy QA and educational projects, thanks to its versatility and its expandability. In this article we would like to analyse the performance reached by the detector in comparison with Geant4 simulations and other kind of dosimeters. In the following paragraphs when we refer to X,Y,Z axis we mean respectively the horizontal axis orthogonal to the beam, the vertical axis orthogonal to the beam and to the beam axis.

2. Materials and methods

2.1 – Machine description

The P.R.O.ME.THE.U.S. machine is based on a stein-less steel structure sustaining a PMMA tank (sizes: 1000 ± 1 mm x 320 ± 1 mm x 215 ± 1 mm) that hosts the mechanics. The mechanical structure uses calibrated steel bars to allow the sliding of the detector head, moved by a 200 steps-per-turn stepping motor. The motion screw step is 4,00 mm ± 0,01 mm. The moving range of the detector head is from 60 mm ± 0,2 mm to 300 mm ± 0,2 mm, making the machine suitable to work with particle beams with widely different energy loss ranges. (For protons in water, from about 85 MeV to 205 MeV.) The detector head includes an horizontal slider (with electric servo control) to adjust the detector position on the X axis. On this second slider a standard DIN rail allows to install the detector box and to adjust the vertical Y position. Thanks to the standard DIN rail, it is possible to change the detector box keeping the original structure unmodified, making this machine expandable for different kinds of measurement. (Fig. 1.0). For our measure, we employed a water resistant 3D printed box hosting a single scintillator, coupled with a silicon

[1] **P**article **R**adiation **O**bserver for **ME**dical **THE**rapy beam characterisation **U**sing computer **S**imulation

photomultiplier (SiPM). The P.R.O.ME.THE.U.S. machine tank can be exposed to the beam also from the opposite direction with respect to the standard one. In this configuration, useful with high energy beams, the mechanical range of movement of the detector head, ranges from 700 mm ± 0,2 mm to 990 mm ± 0,2 mm and an additional horizontal axis could be used to install a beam degrader or a ridge filter. (The operation range could be varied depending upon the specific detector setup).

Figure 1.0 – The P.R.O.ME.THE.U.S. detector seen from above

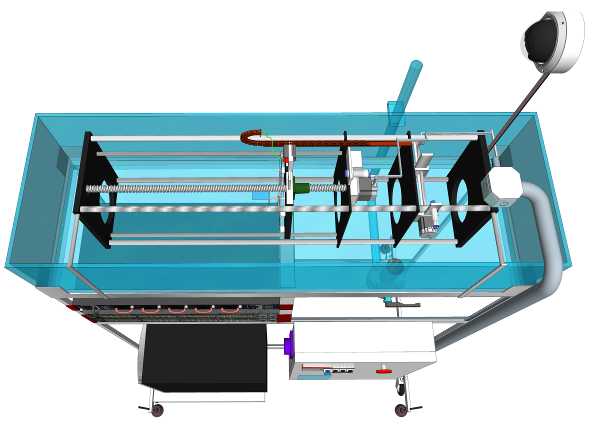

From the electric point of view, the P.R.O.ME.THE.U.S. structure hosts the power distribution system and the Ethernet communication switches and routers on 19” rack guides. The machine hosts also a standard x64 computer that stream the data from the digitizer (CAEN Model DT5720A) via local network, also remotely controlling the Power Supply and Amplification Unit (PSAU) by means of a CAEN Model SP5600. Furthermore, on the structure there is an electric control panel that contains an ARM-based single board computer, the power management electronics, the ADCs for the position sensors and the current limiting MOSFET drivers for the stepping motors.

Figure 2.0 – The P.R.O.ME.THE.U.S. detector (seen on the right) at the Trento proton cyclotron facility (beam line on the left)

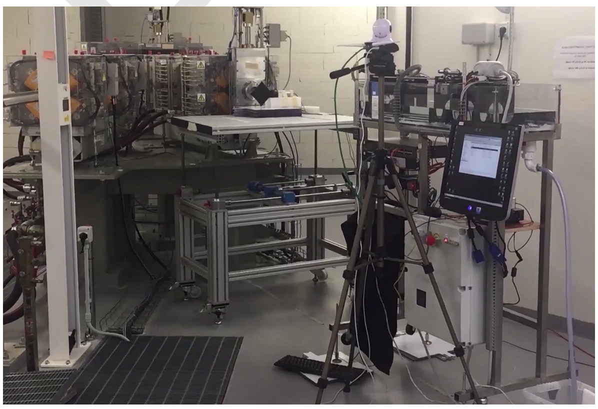

Since the stepping motors are synchronous, the microcontroller always knows the detector head position, because, although the machine is equipped with different absolute sensors that allow for a high precision feedback:
- An inductive proximity sensor (± 0,5 mm) for each motorized axis for homing in and for absolute reference.
- An optical infrared digital distance sensor (± 0,3 mm) on the beam boundary of the Z (beam) axis.
- A resistive potentiometer (± 0,2 mm) providing an absolute position value along the Z axis. This value is saved in a data file and is used to keep track of the energy loss curve.

The detector is equipped with two high-resolution infrared IP cameras, both in the visible and infrared range, allowing researchers to check in real time the correct behaviour of the machine, especially the mechanical positioning system. The cameras include embedded IR light sources to allow operations in completely dark environments, minimizing the light leakages inside the SiPM host box.

2.2 – Scintillator, SiPM detector and electronics

The core of the machine is represented by a 2 mm thick Calcium Fluoride scintillator coupled with a 1.3x1.3 mm^2 silicon photomultiplier by Hamamatsu Photonics (Model MPPC S13360-1350CS) with a thin layer of optic conductive gel, to efficiently optically interface materials with different refraction index. (The mechanical structure is depicted in fig. 3.0). The SiPM detector is soldered on a round shaped PCB, produced by CAEN, that hosts also the temperature sensors needed to feedback the voltage regulator section of the PSAU. By means of the DAQ it’s possible to regulate the dV/dT correction value, to monitor and record temperature variations. The PSAU is connected to the sensor PCB by a cable for the auxiliary signals, while the coaxial cable carrying the detector output reaches a 50Ω passive splitter, feeding the PSAU digital discriminator, for the definition of the trigger signal, and the digitizer, where it is sampled at 250 MSa/s frequency with a 12 bit dynamic range. Then each individual time window is integrated to obtain a value proportional to the energy that the particle lost in the scintillator. (C. del la Taille 2012) (Hamamatsu Photonics K.K. 2016)

Figure 3.0 – Mechanical drawings of the waterproof and lightproof scintillator and SiPM support

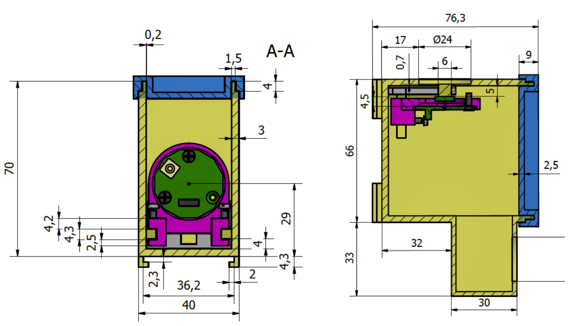

2.3 – The Data Acquisition and slow control software

The software controlling the P.R.O.ME.THE.U.S. detector consists in a suite of different applications running on different workstations, all interconnected by a 1 Gbit/s Ethernet local network, shared between the control room and the experimental apparatus through a dedicated CAT6 cable. A LabView application, designed to regulate the SiPM electrical parameters, allows a quick data quality check to manage the experiment runs. This program generates ASCII files, one for each run, containing a header to specify detector status and complemented with the stepping motor position value and, finally, with the long list of ADC values, measuring the energy loss. A separate program, written in C++ with QT tools (https://www.qt.io/), runs on a different machine which makes the data from the experiment accessible to the control room under the SMB protocol. This allows for a quick, online, data analysis process, providing a plot of the Bragg peak or some run control histograms, using CERN ROOT libraries. Other software tools allow the management of the experiment logbooks and the data backup, while another specific program written in C# with .Net Framework is responsible of the machine control, including the detector positioning along the stepping motor axis.

3. Results

3.1 – CaF_2 scintillator and SiPM test with beta source

The detector, made of a calcium fluoride scintillator coupled with a SiPM, has been tested, prior to the actual data taking, using a low rate ${}^{90}_{38}Sr$ beta source to check the optical coupling and the signal dynamic range. From the test it emerged that the amplitude of the signals produced by the system was strong enough to be directly connected to an output of the passive splitter to the digitizer, thus bypassing the preamplifier. The preamplifier output signal was used for the production of the trigger pulse. (Hamamatsu Photonics K.K. 2016) (V. B. Mikhailik et al. 2006)

3.2 – Description of the test facility

Thanks to the collaboration with the Italian National Institute of Nuclear Physics (INFN) and the Trento Institute of Fundamental Physics and Applications (TIFPA) we could test our detector on the proton beam of the Trento protontherapy centre, a new facility that hosts an IBA Proteus 235 cyclotron that accelerates proton beams up to a maximum energy of 228 MeV. The experiment has been run on the 30° beamline of the irradiation cave that provides a fixed pencil beam in output with an energy range from 70 to 228 MeV and an adjustable beam rate from 10^0 to 10^5 Hz, switchable in a real time upon request. (F. Tommasino et al. 2017) The experiment has been run at the energy of 150 MeV with a fixed particle rate of 10^4 Hz and the absorption liquid used to fill the tank was self-produced deionised water with the following technical specifications, used to set the simulation material:

Table 1 – Deionised water analysis result

Density	1000.3	± 0.2	kg/m^3
Conductivity	0.20	± 0.02	µS/cm
pH @ 20°C	6.98	± 0.01	
Dry residue @ 100°C	000.8	± 0.3	mg/L

3.3 – Scan measurement

The measurement was accomplished in two stages, run at the Trento facility, where the first one was a quick scan of the Z axis: the stepping motor was programmed to run at a fixed, slow speed (we remind that stepping motors are synchronous with the driver signal) during the acquisition. The DAQ was programmed to save the data to a file, organized with a preceding header (containing information such as detector temperature, bias voltages etc…) while individual events were defined as the mean of 50 discrete digitised pulse height values. Aim of the preliminary data taking campaign was to assess, in a such a continuous running mode, the shape and the actual position along the z axis of the Bragg peak. A second step in the data taking, discussed below, was the collection of larger statistics data at individual z positions. Figure 4.0 shows the superposition of these individual, high accuracy, data points with the previous continuous mode acquisition. The noise in the continuous acquisition is significant, but we can appreciate a quite good matching with the more precise, individual, measurements.

Figure 4.0 – P.R.O.ME.THE.U.S. data at 150 MeV with the quick scan curve

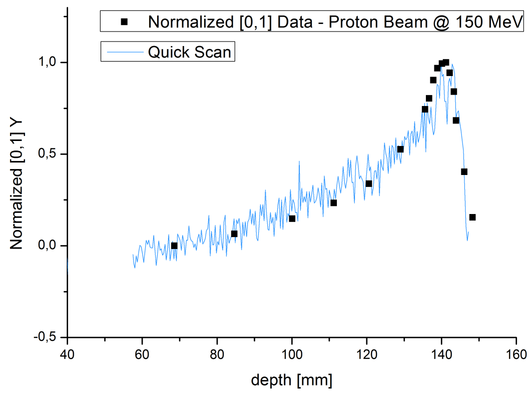

3.4 – Single point measurements

To track the energy loss curve we chose a list of measurement points, not equally distributed along Z, but denser around the Bragg Peak. For each of these we acquired from 800 to 7000 values, where each value is the average of the integration of 50 temporal windows (events). The output values have been reported on a histogram (count vs charge) and then fitted tool using a Gaussian parametrization:

$$f(E,\mu,\sigma) = \frac{1}{\sigma\sqrt{2\pi}}\exp\left(-\frac{(E-\mu)^2}{2\sigma^2}\right) \quad (1)$$

3.5 – Energy loss curve reconstruction

For the reconstruction of the energy loss curve, we represented the points on a (C, z) plane (where C is the charge integrated by the ADC, proportional to the energy lost in the scintillator by the incoming particle). We plot one point for each z measurement: each z value is acquired from the system, while the z error has been estimated from calibration tests (*and turns out to be* $\pm$0,2 mm). The charge and its error arte derived, respectively, from the μ and σ parameters of the Gaussian fit. The obtained graph was then fit using a convoluted Moyal function:

$$f(z) = \frac{\exp\left(-\frac{\left(\frac{-p_4 z - p_0}{p_0} + \exp\left(-p_2 \frac{-p_4 z - p_0}{p_0}\right)\right)}{2}\right) + p_3}{p_1} + p_5 \quad (2)$$

We added, to the standard form of this equation, two additional parameters, p_4 and p_5, representing, respectively, the actual scale of the z axis and the offset of the arbitrary scale of the deposited energy. These additional parameters do not change the function physical meaning, but are only used to adjust the unknown scale factors. In figure 5.0 is shown the fitted raw energy loss curve. ($X^2 / n.d.f. = 0{,}85$)

Figure 5.0 – P.R.O.ME.THE.U.S. raw data at 150 MeV (proton beam) with Moyal fit

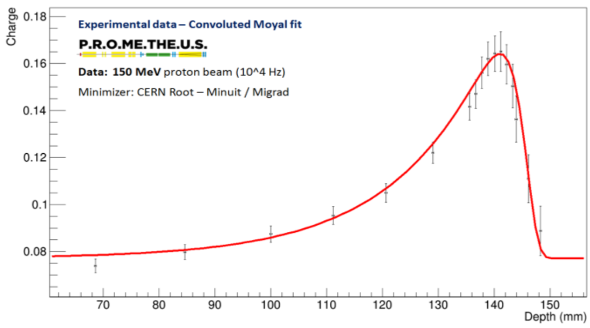

Table 2 – P.R.O.ME.THE.U.S. raw energy loss measurement – proton beam at 150 MeV

Depth [mm] ± 0.2	Mean (μ)	Sigma (σ)	Entries
68.6	12610	503.945	5783
84.6	13600	529.936	5590
100.1	14880	600.249	6587
111.2	16210	638.652	6320
120.6	17830	677.371	7329
129.0	20720	779.973	4828
135.6	24070	972.847	5895
136.7	25000	1029.27	3939
137.8	26530	1144.75	5520
138.9	27530	1223.18	4438
140.1	27910	1275.94	6122
141.2	28020	1439.25	2331
142.2	27140	1426.14	6058
143.3	25560	1588.26	4648
143.9	23140	1667.61	3663
146.1	18830	1732.64	966
148.3	14990	1786.01	810

3.6 – Scintillator quenching correction

Comparing our raw data plot (shown in figure 5.0) with dE/dX Monte Carlo simulation, like the one shown in figure 6.0 or even with a Bragg Peak, measured employing a ionization chamber, we can appreciate a significant discrepancy due to the quenching effects of scintillator detectors (L.L. W. Wang et al 2012) (U. I. Tretyak 2010) that we can correct with the following Birk's empirical formula, where dY/dx is the integrated charge based on the scintillator light yield, dE/dx is the original energy loss, S represents the scintillator efficiency and kB represents the Birk's factor.

$$\frac{dY}{dx} = \frac{S \cdot \frac{dE}{dx}}{1 + kB\,\frac{dE}{dx}} \qquad (3)$$

3.7 – Comparison with simulation

Before the test at the Trento facility, we run a series of simulations using the Geant4 Monte Carlo toolkit. To simplify the simulation setup, we used the LISE++ toolbox to calculate the energy lost in materials along the beam line, before reaching the detector (for example the proton-counting scintillator), then we used, as initial energy for the Geant4 simulation, the beam remaining energy. (O. Tarasov et al. 2002) (T.Aso et al. 2004) In figure 8.0 we represent the superposition of the simulated Bragg Peak with our experimental data. In this case, to obtain an improved matching, we had to modify the original simulated energy loss curve (figure 6.0) to consider the straggling effect induced by the non negligible thickness of the scintillator, its size and its position uncertainties. Figure 7.0 shows the GEANT IV simulation of a beam impinging in water in a continuous way. Our detector, instead, has a finite width, which introduces an additional uncertainty of the actual position where the scintillation signal is generated along z. To take this effect into account we distributed each simulation data point according to a smeared two steps function representing our best knowledge of the scintillator width. The simulation has also been convoluted with another normal distribution simulating the uncertainty on the detector position along the Z axis. The particle gun has been programmed to simulate the interaction of 10^7 particles and the maximum simulation step size of the Monte Carlo engine was of 10^{-3} mm. The histogram bin size was $8{,}0 \cdot 10^{-3}$ mm for the energy loss curve and of $5.0 \cdot 10^{-3}$ for the detector effects convolution distributions. The experimental data shown in figure 8 have been previously corrected from the quenching effects, as it has been explained before.

Figure 6.0 – 150 MeV proton energy loss curve simulated with LISE++ physical simulation software and Gean4 Monte Carlo

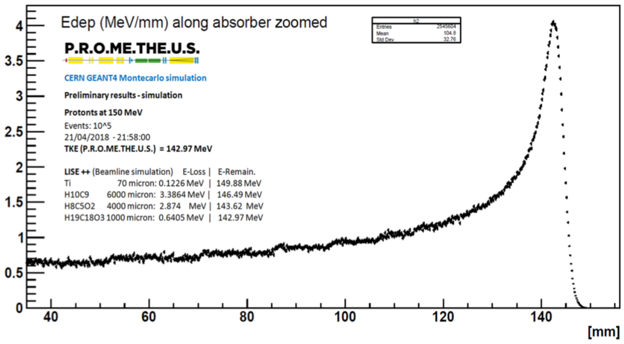

Figure 7.0 – Profile of the scintillation width, used to convolute the Geant4 simulation to include the straggling effects due to the non-negligible thickness and its measured uncertainty (2.00 mm scintillator)

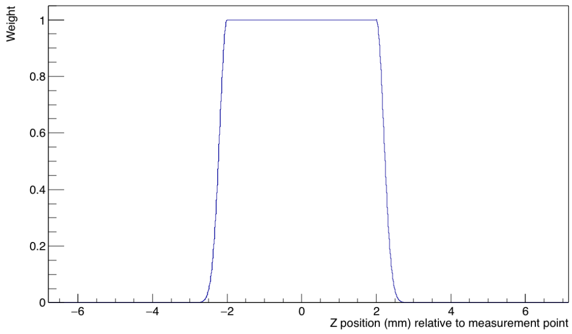

Figure 8.0 – Geant4 simulated Bragg Peak (with scintillator thickness convolution included) and P.R.O.ME.THE.U.S. experimental data (also quenching effect corrected) - (150 MeV proton beam)

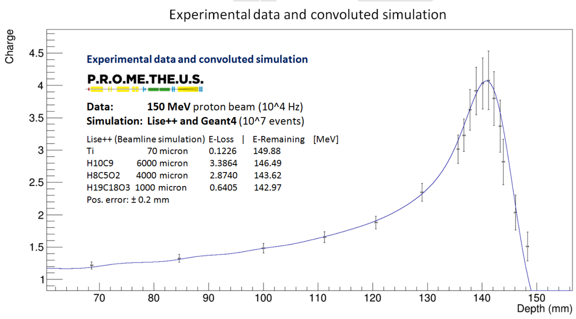

4. Result comparison with other detectors

To evaluate the performances of the P.R.O.ME.THE.U.S. detector we tried to compare the measured energy loss curve to the one measured with a professional IBA Dosimetry Giraffe detector at the same facility and with the same setup. In figure 9.0 it is possible to see the superposition of the two profiles, in blue the one from the IBA detector, in black the one from the P.R.O.ME.THE.U.S, corrected for the scintillator quenching effects. Except for the last two points in the falling edge of the Bragg Peak, where the scintillator detector, working in self-trigger mode with a fixed threshold, could introduce an inefficiency at the lowest energy events, giving a bit higher average value of the dose (see the low entry number for these points in table 2.0), for all the other measurements points the IBA measured value never deviates by more than 1-sigma from the P.R.O.ME.THE.U.S. mean value.

5. Conclusions

The results show that the P.R.O.ME.THE.U.S. detector is able to measure with good approximation the energy loss curve of a proton beam. Our detector explored the possibility to run Bragg Peak measurement employing scintillation detectors that bring several advantages compared to more common ionization chambers. To this extent we can quote a very good signal-noise ratio in a large spectrum of beam rates, the possibility to track single particles, thanks to the quick pulse decay, the good energy resolution and the possibility to employ water-equivalent materials as a detector. In our setup we coupled the scintillator with a silicon photomultiplier (SiPM) which, compared to classic PMT tubes, provides additional advantages like: (SensL. 2011)

- High voltage power supply is not required
- A high event acquisition rate
- Very good signal / noise ratio (further improvable using a coincidence trigger detector)
- Improved resistance to magnetic field effects

Furthermore, this kind of setup does not require expensive electrometers for signal readout, like ionizing chambers. Finally, the P.R.O.ME.THE.U.S. detector was not meant to be used for very high precision characterisations, but considering its relatively low cost, its unexpectedly good performances, this opens up new scenarios in educational projects and for case studies of scintillators and SiPMs behaviours in Bragg Peak QA applications.

Figure 9.0 – P.R.O.ME.THE.U.S. experimental data compared with IBA Giraffe detector result, measured both at TIFPA facility. (Proton beam, energy at the detector entrance: 143 MeV)

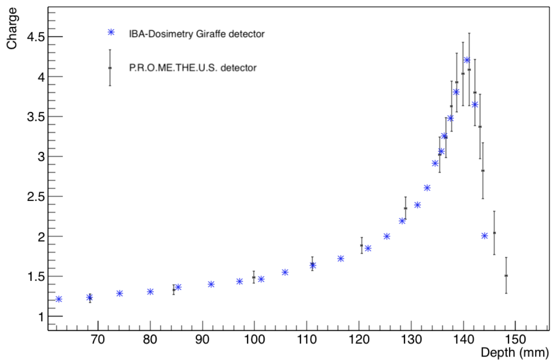

6. Future upgrades

The P.R.O.ME.THE.U.S. design is widely expandable, some possible future upgrades include new sensors (also for beam imaging) and new detectors that can be connected to the free narrow-band channels on the logic board ADC, or to the free broad-band channels of the digitizer ADC. To increase the Z positioning precision, we plan to replace the resistive resolver sensor with a laser distance sensor, that allow an on-board setup of the voltage scaling, removing the need for a Z axis calibration. Another important step is the upgrade of the software suite, integrating all the programs in a unique control interface that dialogues with the machine via Internet through a VPN tunnel, allowing a completely remote management of the machine, the possibility to run (also remotely) totally automated single click measurements and opening new collaboration scenarios. In the future, for example, student groups could access the control software participating to data acquisition in collaboration with scientist teams, interacting through the live cameras and the web shared control interface.

7. Acknowledgement

This study has been made possible only thanks to the collaboration of the Italian National Institute of Nuclear Physics (INFN), especially the researchers from the departments of Milano Bicocca (Dr. Dario Menasce) and Torino (Dr. Nadia Pastrone). Special thanks to the Università degli Studi dell'Insubria for the indispensable technical support, for the experiment coordination and for the test with radioactive sources, in particular thanks to Dr. Massimo Caccia, Dr. Romualdo Santoro, Dr. Samuela Lomazzi. We are also grateful to the Trento Institute for Fundamental Physics and Applications and the Trento protontherapy centre for making possible our experiment in their proton beam facility, in particular thanks to Dr. Marco Durante, Dr. Francesco Tommasino, Dr. Marta Rovituso and Dr. Christian Manea. Thanks to CAEN s.p.a. for providing the PSAU and Digitizer electronics and to Dr. Cristina Mattone for the technical support. We finally acknowledge CERN for the "Beamline for School" initiative that introduced us to this project.

8. Funding

This work has been done thanks to the funds of the IIS Nicola Pellati Scientific High School, the Italian National Institute of Nuclear Physics (INFN) and the sponsorship of CAEN s.p.a., Phoenix PCB s.r.l., PAT s.r.l., U.T.I. s.r.l. The total expense for the detector material is estimated around €7000.

9. References

C. del la Taille. 2012. "SiPM electronics overview." Photodet Conference. IN2P3 - Institut national de physique nucléaire et de physique des particules.

C.R. Gruhn. 2010. "BRAGG CURVE SPECTROSCOPY." INS International Conference on Radiation Detectors. Tokyo: Lawrence Berkeley National Laboratory. 1-8.

F. Tommasino et al. 2017. "Proton beam characterization in the experimental room of the Trento Proton Therapy facility." Nuclear Instruments and Methods in Physics Research, A 869: 15-17.

Hamamatsu Photonics K.K. 2016. "Multi-Pixel Photon Counter S13360 series." Accessed June 2018. https://www.hamamatsu.com/resources/pdf/ssd/s13360_series_kapd1052e.pdf.

I. Dattner et al. 2011. "On deconvolution of distribution functions." The Annals of Statistics (Institute of Mathematical Statistics).

L. L. W. Wang et al. 2012. "Determination of the quenching correction factors for plastic scintillation detectors in therapeutic high-energy proton beams." Physics in Medicine & Biology (IOP Science).

L. Moneta. 2015. "Statistical Software Tools RooFit/RooStats." Terascale Statistics School 2015.

McParland, Di Brian J. 2010. Nuclear Medicine Radiation Dosimetry: Advanced Theoretical Principles. Springer.

O. Tarasov et al. 2002. "The code LISE: a new version for "Windows"." Nuclear Physics A 701: 661-665.

P. Eckert et al. 2010. "Characterisation studies of silicon photomultipliers." Nuclear Instruments and Methods in Physics Research, A 620.

S. M. Vatnitsky et al. 1999. "Dosimetry techniques for narrow proton beam radiosurgery." Physics in Medicine & Biology 44: 1-3.

SensL. 2011. "Introduction to SiPM - TECHNICAL NOTE." Accessed 2018. https://www.sensl.com/downloads/ds/TN%20-%20Intro%20to%20SPM%20Tech.pdf.

T. Davidek et al. 1997. "Parametrization of the Muon Response in the Tile Calorimeter." Nuclear Centre of the Faculty of Mathematics and Physics, Charles University, Prague.

T.Aso et al. 2004. "Verification of the Dose Distributions with GEANT4 Simulation for Proton Therapy." IEEE Symposium Conference Record Nuclear Science 2004. IEEE. 2-4.

The Qt Company. n.d. Qt - Cross-platform software development for embedded. Accessed August 2018, 2018. https://www.qt.io/.

U. I. Tretyak. 2010. “Semi-empirical calulation of quenching factors for ions in scintillators.” Astroparticle Physics 33: 40-53.

V. B. Mikhailik et al. 2006. “Scintillation properties of pure CaF2.” Nuclear Instruments and Methods in Physics Research, A 566: 522-524.